

Supplements to “A Critical Supermassive Black Hole Mass Regulating Galaxy Evolution”

1 Galaxy Formation Modelling

The main strategy behind the modelling approach we follow is to first calculate the collapse and merging history of individual dark matter halos, which is governed purely by gravitational interactions, and secondly to calculate the more complex physics of the baryons inside these dark matter halos, including e.g. radiative cooling of the gas, star formation and feedback from supernovae by simplified prescriptions on top of the dark matter evolution. Each of the dark matter halos consist of three main components which are distributed among individual galaxies inside them. A stellar, cold and hot gas component, where the latter is only attributed to *central* galaxies, the most massive galaxies inside individual halos. In the following sections, we will describe briefly the recipes used to calculate these different components which are mainly based on recipes presented in Kauffmann et al.¹ (hereafter, K99) and Springel et al.² (hereafter, S01), and we refer readers for more details on model implementations to their work and references therein.

Throughout this paper we use the following set of cosmological parameters: $\Omega_0 = 0.3$, $\Omega_\Lambda = 0.7$, $\Omega_b/\Omega_0 = 0.15$, $\sigma_8 = 0.9$ and $h = 0.65$.

Dark Matter Evolution We calculate the merging history of dark matter halos according to the prescription presented in Somerville et al.³. This approach has been shown to produce merging histories and progenitor distributions in reasonable agreement with result from N-body simulations

of cold dark matter structure formation in a cosmological context⁴. The merging history of dark matter halos is reconstructed by breaking each halo up into progenitors above a limiting minimum progenitor mass M_{min} . This mass cut needs to be chosen carefully as it ensures that the right galaxy population and merging histories are produced within the model. Progenitor halos with masses below M_{min} are declared as *accretion* events and their histories are not followed further back in time. Progenitors labelled as accretion events should ideally not host any significant galaxies in them and be composed mainly of primordial hot gas at the progenitor halo's virial temperature. To achieve a good compromise between accuracy and computational time, we use $M_{min} = 10^{10} M_{\odot}$, which ensures that the results presented here are unaffected by numerical resolution effects.

Baryonic Physics As mentioned above, once the merging history of the dark matter component has been calculated, it is possible to follow the evolution of the baryonic content in these halos forward in time. We assume each halo consists of three components: hot gas, cold gas and stars, where the latter two components can be distributed among individual galaxies inside a single dark matter halo. The stellar components of each galaxy are further divided into bulge and disc, to allow morphological classifications of model galaxies. In the following, we describe how the evolution of each component is calculated.

Gas Cooling & Reionisation Each branch of the merger tree starts at a progenitor mass of M_{min} and ends at a redshift of $z = 0$. Initially, each halo is occupied by hot primordial gas which was captured in the potential well of the halo and shock-heated to its virial temperature $T_{vir} = 35.9 [V_c / (\text{km s}^{-1})]^2$ K, where V_c is the circular velocity of the halo^{1,5}. Subsequently this hot gas

component is allowed to radiatively cool and settles down into a rotationally supported gas disc at the centre of the halo, which we identify as the central galaxy⁵⁻⁷. The rate at which hot gas cools down is estimated by calculating the cooling radius inside the halo using the cooling functions provided by⁸ and the prescription in S01. In the case of a merger between halos we assume that all of the hot gas present in the progenitors gets shock-heated to the virial temperature of the remnant halo, and this gas can cool down only onto the new central galaxy which is the central galaxy of the most massive progenitor halo. The central galaxy of the less massive halo will become a satellite galaxy orbiting inside the remnant halo. In this way, a halo can host multiple satellite galaxies, depending on the merging history of the halo, but will always only host one central galaxy onto which gas can cool. The cold gas content in satellite galaxies is given by the amount present when they first became satellite galaxies and does not increase, but decreases due to ongoing star formation and supernova feedback.

In the simplified picture adopted above, the amount of gas available to cool down is limited only by the universal baryon fraction $\Omega_b h^2 = 0.0224^9$. However, in the presence of a photoionising background the fraction of baryons captured in halos is reduced^{10,11} and we use the recipe of Somerville et al.¹², which is based on a fitting formulae derived from hydrodynamical simulations¹¹, to estimate the amount of baryons in each halo. For the epoch of reionisation, we assume $z_{reion} = 20$, which is in agreement with observations of the temperature-polarisation correlation of the cosmic microwave background¹³.

Star Formation in Discs and Supernova Feedback Once cooled gas has settled down in a disc, we allow for fragmentation and subsequent star formation according to a parameterised global Schmidt-Kennicutt law¹⁴ of the form $\dot{M}_* = \alpha M_{cold}/t_{dyn,gal}$, where α is a free parameter describing the efficiency of the conversion of cold gas into stars, and $t_{dyn,gal}$ is assumed to be the dynamical time of the galaxy and is approximated to be 0.1 times the dynamical time of the dark matter halo¹. As in K99 we allow star formation only in halos of $V_c < 350$ km/s to avoid excessively-massive central galaxies in clusters.

Feedback from supernovae plays an important role in regulating star formation in small mass halos and in preventing excessively-massive satellite galaxies from forming. We implement feedback based on the prescription presented in K99 with

$$\Delta M_{reheat} = \frac{4}{3} \epsilon \frac{\eta_{SN} E_{SN}}{V_c^2} \Delta M_*. \quad (1)$$

Here we introduce a second free parameter ϵ which represents our ignorance about the efficiency with which the energy from supernovae reheats the cold gas. The expected number of supernovae per solar mass of stars formed is given by $\eta_{SN} = 5 \times 10^{-3}$, taken as the value for the Scalo initial mass function¹⁵, and $E_{SN} = 10^{51}$ erg is the energy output from each supernova. We take V_c as the circular velocity of the halo in which the galaxy was last present as a central galaxy.

Galaxy Mergers We allow for mergers between galaxies residing in a single halo. As mentioned earlier, each halo is occupied by one central galaxy and a number of satellite galaxies depending on the past merging history of the halo. Whenever two halos merge, the galaxies inside them are going to merge on a time-scale which we calculate by estimating the time it would take the satellite

to reach the centre of the halo under the effects of dynamical friction. Satellites are assumed to merge only with central galaxies and we set up their orbits in the halo according to the prescription of K99, modified to use the Coulomb logarithm approximation of S01.

If the mass ratio between the two merging galaxies is $M_{gal,1}/M_{gal,2} \leq 3.5$ ($M_{gal,1} \geq M_{gal,2}$) we declare the event as a *major* merger and the remnant will be an elliptical galaxy and the stellar components and the gas will be treated according to the prescriptions below. In the case of *minor* merger $M_{gal,1}/M_{gal,2} > 3.5$ the cold gas in the disc of the smaller progenitor is assumed to settle down in the gas disc of the remnant and its stars contribute to the bulge component of the remnant¹.

Formation of Ellipticals and Bulges It is suggested that major mergers will lead to the formation of elliptical galaxies¹⁶. Indeed detailed numerical simulations in the last decade seem to support this hypothesis^{17,18}, and we will assume in the following that major mergers disrupt the discs in progenitor galaxies as seen in various numerical simulations and relax to a spheroidal distribution. During the merger, any cold gas in the discs of the progenitor galaxies is assumed to be funnelled into the centre of the remnant where it ignites a starburst which transforms all of the cold gas into stars contributing to the spheroidal component^{1,2}. The second assumption is certainly a simplification of what might happen since we neglect the possibility that not all of the cold gas is funnelled to the centre but some fraction of it may for example settle down onto an extended disk which continues to grow inside-out by fresh supply of gas from tidal tails^{19–22}. The results of Barnes²² indicate that 40% – 80% of the initial gas in the disc could end up in the central region of the remnant and be consumed in a starburst. The exact amount is somewhat dependent on the merger geometry

and on the mass ratio of the merger. Unfortunately, a sufficiently large survey investigating the gas inflow to the centres of merger remnants is not available yet, so we use the simplified approach of assuming that all cold gas gets used up in the central starburst. This prescription for the fate of the cold gas results in an overestimate of the spheroid masses and an underestimate of the secondary disc components in our model. This is not very significant for massive ellipticals since they are mainly formed in relatively non-dissipative mergers²³.

Formation and Growth of Super-Massive Black Holes We here follow the model introduced in Kauffmann & Haehnelt²⁴ in which super-massive black holes get formed and fed during major mergers of galaxies. The assumption is to say that a fraction of the the cold gas available in the progenitor discs, that is funnelled into the centre of the remnant, will be accreted onto the black hole. Kaufmann & Haehnelt introduced the following scaling law for the effectiveness of this process:

$$\dot{M}_{\bullet} = \frac{f_{bh} M_{cold}}{1 + (280 \text{ km s}^{-1} / V_c)^2}, \quad (2)$$

where M_{cold} is the amount of cold gas available in the progenitor disks, V_c the circular velocity of the dark matter halo and f_{bh} a free parameter. This scaling provides a good fit to the observed relation between the mass of the super-massive black hole and the velocity dispersion of a galaxy²⁴. Following Croton et al.²⁵ we here assume the velocity dispersion of a galaxy to be identical to the circular velocity of the dark halo the galaxy is embedded in. This however is not strictly true as e.g. in the case of an isothermal sphere $V_c / \sigma = \sqrt{2}$. Several authors have investigated the correlation between V_c and σ ^{26,27} and found different correlations. We here note that using a different scaling between V_c and σ in our models still produces the same $M_{\bullet} - \sigma$ -relation if we adjust the free

parameter f_{bh} accordingly.

Feedback from Super-Massive-Black Holes We here introduce a new prescription for the modelling of feedback from super-massive black holes, which is based on the results presented in this paper. According to our analyses a critical black hole mass exists for a given galaxy velocity dispersion σ , at which feedback is so strong that it reheats all the available cold gas and hence prevents further star formation. This critical black hole mass is derived from our empirical fit to the residual star formation fraction found in our data as

$$M_{\bullet,c} = 1.26 \times 10^8 \left(\frac{\sigma}{200} \right)^{3.65} \quad (3)$$

In galaxies with black holes more massive than the corresponding critical black hole mass we stop any cooling of gas and star formation. We calibrate this relation to give the right fraction of RSF galaxies as seen in Figure 1.

Free Parameters We normalise our two model parameters for the star formation efficiency α and supernova feedback efficiency η by matching the I -band Tully-Fisher relation of Giovanelli et al.²⁸ and requiring that spiral central galaxies of halos with circular velocity $V_C = 220$ km/s have on average $10^{11} M_{\odot}$ of stars and $10^9 M_{\odot}$ of cold gas²⁹. The third free parameter f_{bh} , which regulates the black hole growth is set to match the observed $M_{\bullet} - \sigma$ -relation and is $f_{bh} = 0.02$.

2 The Virgo Cluster Data

We derive the $NUV - V$ colour- σ relation for the Virgo cluster down to much smaller values of σ than in our GALEX-SDSS sample by combining the near-UV and optical photometry from Boselli et al.³⁰ with velocity dispersion measurements from the GOLDmine database³¹. The purpose of looking at the Virgo cluster galaxies is to constrain the low end of the σ and so get an idea of the point at which all galaxies are RSF galaxies and thus below critical. Since the optical photometry of the Virgo galaxies in this sample are in V-band, we approximately convert the RSF criterion of $NUV-r=5.4$ to $NUV-V$. We use simple stellar populations of solar metallicity and three ages (3,6 and 9 Gyr) to derive the $NUV-V$ RSF criterion; these are $NUV-V= 5.16, 5.12$ and 5.09 respectively. In all three cases, the point at which no Virgo early-type galaxy is above this cutoff - i.e. all show some signs of young populations - is at $\sigma \sim 80 km s^{-1}$.

3 The RSF criterion

We use $NUV-r$ colour as a discriminant between those galaxies which are quiescent and those which show signs of recent star formation. Besides AGN, there is one further effect which can mimic young stars in the near-UV. Extremely old stellar populations can give rise to the UV upturn phenomenon in some early-type galaxies^{32,33}. We choose the $NUV-r$ colour of one of the strongest UV upturn galaxies NGC 4552³³ to be the boundary between galaxies with no young component on the one hand and those that are so blue they must have some young stars in them. Although still quite limited, theoretical population synthesis models which are supported by empirical data

(Lee et al.³⁴) also suggest that the NUV-r of passively evolving ETGs could not be much bluer than 5.4. Using this criterion, we compute the fraction of galaxies that must have experienced some star formation within the last billion years. The ages and mass fractions of these young stellar components are generally 300-500 Myr and 1-3% by mass³⁵. Due to the high sensitivity to dust extinction, these fractions are a lower limit as cold gas and dust have been detected in many early-type galaxies^{36,37}. *NUV-r* probes recent star formation for up to 1 Gyr and so traces different time scales than those of AGN feedback. so there may be a certain amount of time lag between the UV emissions and the processes underlying feedback.

4 Visual Inspection of Galaxy Morphology

The process and criteria of the visual inspection are described in detail in Schawinski et al.³⁸. In summary, we find early-type galaxy (ETG) candidates from the SDSS database using *frac_Dev* parameter, which is the weight of the de Vaucouleurs component in the two-component (de Vaucouleurs and exponential disc) fits. We use $frac_Dev > 0.95$, which is a highly conservative criterion, hoping to exclude as many spiral interpolers as possible. Despite this, still some spiral bulges remain in our sample. Hence, we remove them via visual inspection on *gri* bands³⁹. Since visual inspections are also subject to errors, we investigate out to what redshift and apparent magnitude visual inspection based on SDSS images is reliable by comparing them with one of the COMBO-17 fields overlapping SDSS. The COMBO-17 image is significantly deeper and has much better seeing with 0.7'' as opposed to 1.4'' which are typical for SDSS. By comparing our classification based on these two different data sets, we concluded that visual inspection of mor-

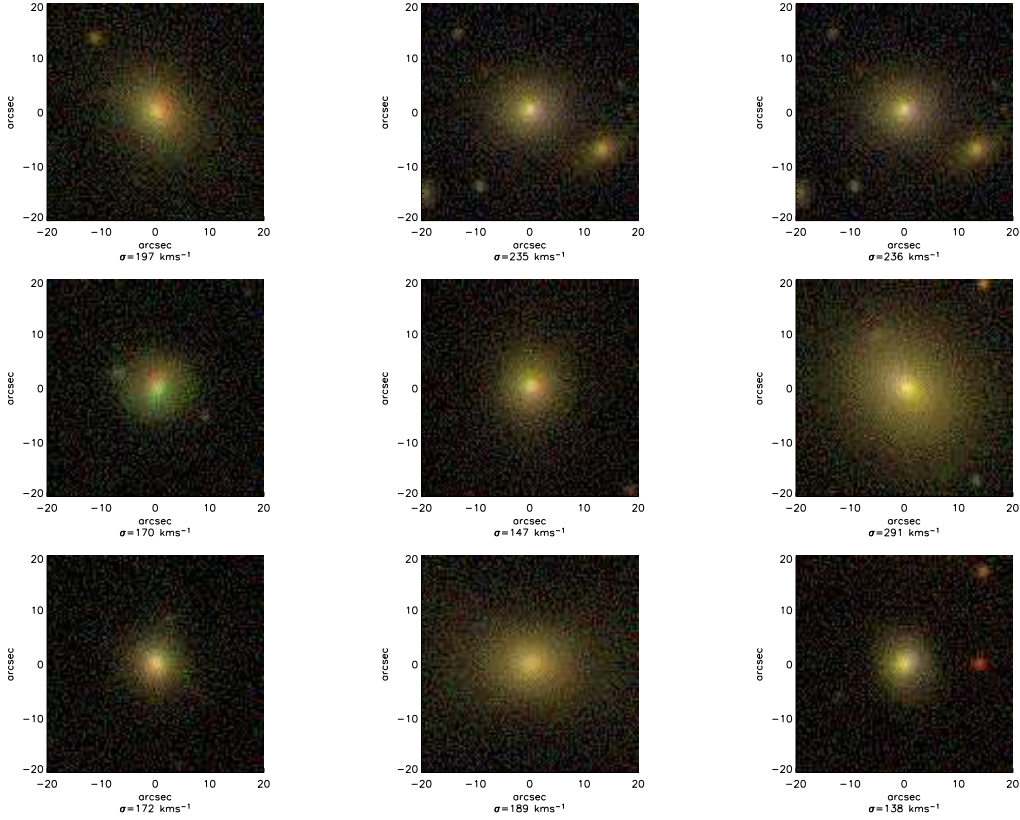


Figure 1: Example galaxies from our SDSS sample. The images are gri composites³⁹ and span a wide range in velocity dispersion.

phology using SDSS was possible to $z \sim 0.13$ and $R < 17.31$. We settle on more conservative limits of $z < 0.1$ and $r < 16.8$. The presence of late-type interlopers with star-forming disks or spiral arms is therefore not a significant concern and does not give rise to the correlations between M_r , σ and NUV-r color. A selection of sample images with their velocity dispersions are shown in Figure 1.

1. Kauffmann, G., Colberg, J. M., Diaferio, A. & White, S. D. M. Clustering of galaxies in a hierarchical universe - I. Methods and results at $z=0$. *Mon. Not. R. Astron. Soc.* **303**, 188–206

- (1999).
2. Springel, V., White, S. D. M., Tormen, G. & Kauffmann, G. Populating a cluster of galaxies - I. Results at $z=0$. *Mon. Not. R. Astron. Soc.* **328**, 726–750 (2001).
 3. Somerville, R. S. & Kolatt, T. S. How to plant a merger tree. *Mon. Not. R. Astron. Soc.* **305**, 1–14 (1999).
 4. Somerville, R. S., Lemson, G., Kolatt, T. S. & Dekel, A. Evaluating approximations for halo merging histories. *Mon. Not. R. Astron. Soc.* **316**, 479–490 (2000).
 5. White, S. D. M. & Frenk, C. S. Galaxy formation through hierarchical clustering. *Astrophys. J.* **379**, 52–79 (1991).
 6. Silk, J. On the fragmentation of cosmic gas clouds. I - The formation of galaxies and the first generation of stars. *Astrophys. J.* **211**, 638–648 (1977).
 7. White, S. D. M. & Rees, M. J. Core condensation in heavy halos - A two-stage theory for galaxy formation and clustering. *Mon. Not. R. Astron. Soc.* **183**, 341–358 (1978).
 8. Sutherland, R. S. & Dopita, M. A. Cooling functions for low-density astrophysical plasmas. *Astrophys. J. Supp.* **88**, 253–327 (1993).
 9. Spergel, D. N. *et al.* First-Year Wilkinson Microwave Anisotropy Probe (WMAP) Observations: Determination of Cosmological Parameters. *Astrophys. J. Supp.* **148**, 175–194 (2003).
 10. Navarro, J. F. & Steinmetz, M. The Effects of a Photoionizing Ultraviolet Background on the Formation of Disk Galaxies. *Astrophys. J.* **478**, 13–28 (1997).

11. Gnedin, N. Y. Effect of Reionization on Structure Formation in the Universe. *Astrophys. J.* **542**, 535–541 (2000).
12. Somerville, R. S. Can Photoionization Squelching Resolve the Substructure Crisis? *Astrophys. J. Lett.* **572**, L23–L26 (2002).
13. Kogut, A. *et al.* First-Year Wilkinson Microwave Anisotropy Probe (WMAP) Observations: Temperature-Polarization Correlation. *Astrophys. J. Supp.* **148**, 161–173 (2003).
14. Kennicutt, R. C. The Global Schmidt Law in Star-forming Galaxies. *Astrophys. J.* **498**, 541–552 (1998).
15. Scalo, J. M. The stellar initial mass function. *Fundamentals of Cosmic Physics* **11**, 1–278 (1986).
16. Toomre, A. & Toomre, J. Galactic Bridges and Tails. *Astrophys. J.* **178**, 623–666 (1972).
17. Barnes, J. E. & Hernquist, L. Dynamics of interacting galaxies. *Ann. Rev. Astron. Astrophys.* **30**, 705–742 (1992).
18. Burkert, A. & Naab, T. Major Mergers and the Origin of Elliptical Galaxies. *LNP Vol. 626: Galaxies and Chaos* **626**, 327–339 (2003).
19. Barnes, J. E. & Hernquist, L. E. Fueling starburst galaxies with gas-rich mergers. *Astrophys. J. Lett.* **370**, L65–L68 (1991).
20. Mihos, J. C. & Hernquist, L. Gasdynamics and Starbursts in Major Mergers. *Astrophys. J.* **464**, 641–663 (1996).

21. Barnes, J. E. Gas Dynamics in Galaxy Mergers. In *ASP Conf. Ser. 240: Gas and Galaxy Evolution*, 135 (2001).
22. Barnes, J. E. Formation of gas discs in merging galaxies. *Mon. Not. R. Astron. Soc.* **333**, 481–494 (2002).
23. Khochfar, S. & Burkert, A. The Importance of Spheroidal and Mixed Mergers for Early-Type Galaxy Formation. *Astrophys. J. Lett.* **597**, L117–L120 (2003).
24. Kauffmann, G. & Haehnelt, M. G. The clustering of galaxies around quasars. *Mon. Not. R. Astron. Soc.* **332**, 529–535 (2002).
25. Croton, D. J. *et al.* The many lives of agn: cooling flows, black holes and the luminosities and colours of galaxies *Mon. Not. R. Astron. Soc.* **365**, 11–28 (2006).
26. Ferrarese, L. Beyond the Bulge: A Fundamental Relation between Supermassive Black Holes and Dark Matter Halos. *Astrophys. J.* **578**, 90–97 (2002).
27. Pizzella, A. *et al.* On the Relation between Circular Velocity and Central Velocity Dispersion in High and Low Surface Brightness Galaxies. *Astrophys. J.* **631**, 785–791 (2005).
28. Giovanelli, R. *et al.* The Tully-Fisher Relation and H_0 . *Astrophys. J. Lett.* **477**, L1–L4 (1997).
29. Somerville, R. S. & Primack, J. R. Semi-analytic modelling of galaxy formation: the local Universe. *Mon. Not. R. Astron. Soc.* **310**, 1087–1110 (1999).
30. Boselli, A. *et al.* UV Properties of Early-Type Galaxies in the Virgo Cluster. *Astrophys. J. Lett.* **629**, L29–L32 (2005).

31. Gavazzi, G., Boselli, A., Donati, A., Franzetti, P. & Scodreggio, M. Introducing GOLDMine: A new galaxy database on the WEB. *Astron. Astrophys.* **400**, 451–455 (2003).
32. Code, A. D. & Welch, G. A. Ultraviolet photometry from the Orbiting Astronomical Observatory. XXVI - Energy distributions of seven early-type galaxies and the central bulge of M31. *Astrophys. J.* **228**, 95–104 (1979).
33. Burstein, D., Bertola, F., Buson, L. M., Faber, S. M. & Lauer, T. R. The far-ultraviolet spectra of early-type galaxies. *Astrophys. J.* **328**, 440–462 (1988).
34. Lee, Y.-W. *et al.* The Look-back Time Evolution of Far-Ultraviolet Flux from Elliptical Galaxies: The Fornax Cluster and A2670. *Astrophys. J. Lett.* **619**, L103–L106 (2005).
35. Kaviraj, S. UV-optical colours as probes of early-type galaxy evolution (in prep.).
36. Knapp, G. R., Guhathakurta, P., Kim, D.-W. & Jura, M. A. Interstellar matter in early-type galaxies. I - IRAS flux densities. *Astrophys. J. Suppl.* **70**, 329–387 (1989).
37. Temi, P., Brighenti, F., Mathews, W. G. & Bregman, J. D. Cold Dust in Early-Type Galaxies. I. Observations. *Astrophys. J. Suppl.* **151**, 237–269 (2004).
38. Schawinski, K. *et al.* The effect of environment on the UV colour-magnitude relation of early-type galaxies. *ArXiv Astrophysics e-prints* (2006). arXiv:astro-ph/0601036.
39. Lupton, R. *et al.* Preparing Red-Green-Blue Images from CCD Data. *Publications of the Astronomical Society of the Pacific* **116**, 133–137 (2004).